

The Dominant T Wave and Its Significance

ADRIAAN VAN OOSTEROM, PH.D.

From the Department of Medical Physics, University of Nijmegen, Nijmegen, The Netherlands

The Dominant T Wave. Introduction: The shapes of the T waves as observed in different leads placed on the thorax are very similar. The dominant T wave is introduced as a means to characterize this general signal shape. Its relationship to the transmembrane potentials of cardiac myocytes is discussed.

Methods and Results: The source description of a biophysical model that previously was shown to yield realistic T waveforms was analyzed in order to exploit its relation to the transmembrane potentials of the cardiac myocytes at the surface bounding the myocardium. The product of this analysis is the dominant T wave: a waveform that describes the slope of the transmembrane potential. It is shown that the dominant T wave can be estimated easily from the matrix of sampled lead potentials. The timing of its peak reveals the mean of the repolarization times of the involved transmembrane potentials. The amplitude of the peak is the maximum downward slope of the transmembrane potential. This amplitude is independent of the volume conductor effects of the tissues surrounding the heart. The estimate of the dominant T wave retains this property.

Conclusion: The dominant T wave reflects the derivative of the recovery phase of a generalized transmembrane potential. Its amplitude is independent of the volume conductor properties of the tissues surrounding the heart. This is a unique feature that greatly facilitates the interpretation and application of the other signal features of the dominant T wave. (*J Cardiovasc Electrophysiol*, Vol. 14, pp. S180-S187, October 2003, Suppl.)

dominant T wave, repolarization dispersion

Introduction

When looking at T waves recorded by multiple leads placed on the thorax, the striking feature is that, apart from differences in timing, sign, and amplitude of the observed signals, their waveforms are quite similar. This holds true irrespective of the particular lead system used: the standard 12-lead system or any other lead system involving a larger or a smaller number of electrodes. In healthy subjects, the variation in the observed waveforms of all leads may be very small. An example of this is shown in Figure 1, which depicts the 64 QRST waveforms observed in a healthy subject.

In contrast, the standard deviations of comparable signals pertaining to T waves in various types of cardiac disease tend to be much greater. This observation has led to the exploration of features expressing the dominance of one of the signal components hidden in the ensemble of observed signals over that of other components.¹ The appropriate tool here is the singular value decomposition (SVD) of the matrix representing all lead signals (rows of the matrix) at all sampling points in time (columns of the matrix). This method is equivalent to principal component analysis, the Karhunen-Loeve expansion of signals, and factor analysis. If the spectrum of successive singular values exhibits a steep downward slope from its first dominant value onward, the data may be approximated well by using the corresponding dominant principal component (signal). The ratio of the first singular value to the sum of all singular values indicates how well the data

can be represented by taking just the first term. This ratio has been studied for its potential to quantify abnormal repolarization.¹

van Oosterom² provided an explanation for this SVD approach to the T wave, derived from a biophysical model of the genesis of the T wave, the same model used in this article. The model was documented in detail by van Oosterom.³ The model describes the genesis of the T wave as a linear combination of a collection of transmembrane potentials. An early application of this concept can be found in the work of Harumi et al.⁴ They demonstrated that T waves appear after subtracting just two stylized transmembrane waveforms, each having a slightly different timing. After an initially seemingly unfounded use of this concept while modeling the T wave,⁵ a formal justification came out of the work of Geselowitz.^{6,7} The idea was applied by di Bernardo and Murray⁸ and independently worked out in detail in a publication³ that formed the inspiration for the current article.

This article introduces the dominant T wave, a concept that was implied in previous work,³ and its relationship with the downward slope of the transmembrane potentials of the myocytes at the surface bounding the ventricles. It describes a simple way of computing the dominant T wave, as well as its relationship with various features of T waves observed on the body surface. The latter T waves will be referred to as the "common" T waves, T_{com} .

The article is organized as follows. First, the biophysical model that provides the basis for the subsequent introduction of the dominant T wave is summarized. Next, the dominant T wave is defined, and it is shown how it can be computed from observed ECGs. Finally, various interpretations of the properties of the dominant T wave are presented. The intermediate steps taken are expressed most efficiently by using the notations from linear algebra (mainly just a matrix multiplication). These steps are included in Appendices A to D.

Address for correspondence: Adriaan van Oosterom, Ph.D., Department of Medical Physics, University of Nijmegen, Geert Grooteplein 21, 6525EZ, Nijmegen, The Netherlands. Fax: 31-24-3541435; E-mail: avo@mbfys.kun.nl

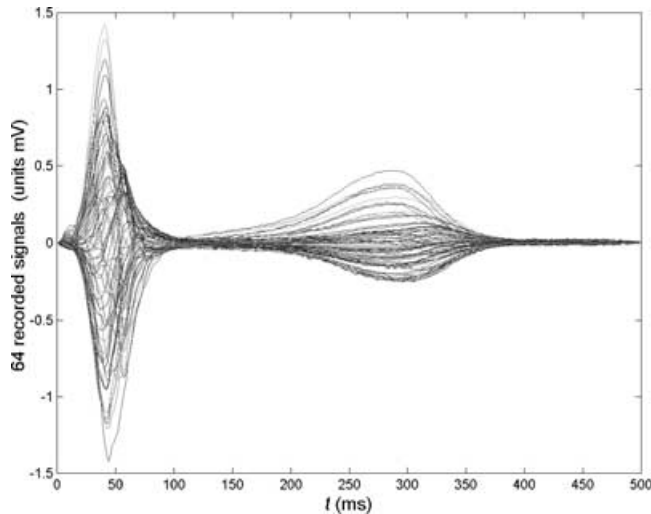


Figure 1. Collection of 64 simultaneous QRST waveforms recorded from a healthy subject. The signals are shown superimposed in order to stress the general similarities between the ST-T waveforms.

Theory

The Biophysical Model

A general formulation for the genesis of ECG waveforms as observed on the body surface reads:

$$\Phi = AS. \tag{1}$$

In this formulation, a matrix multiplication, matrix S , represents the strengths of the current sources generating the body surface potentials. Row n ($n = 1, N$) represents the time course at T discrete time instants of source element n . The nature of these source elements may be quite different. In the case of the classic dipole, the basis of vector cardiography, just $N = 3$, source elements are considered: the components of the vector in three-dimensional space. In the source model used in this article, numerous source elements are postulated, located at a set of evenly distributed nodes specifying the closed surface S_h bounding ventricular mass: endocardium, epicardium, and their connection at the base of the ventricles. To the source strengths at each of these nodes are assigned the time courses of the transmembrane potentials of nearby myocytes. The transmembrane potential at node n acts as the local strength of an elementary double-layer element. This source element may be likened to a current dipole normal to the local surface S_h , with its strength also proportional to the area of S_h represented by the node.

Matrix Φ represents the potentials observed on the body surface. Its row l ($l = 1, L$) represents the ECG at lead l , sampled at T consecutive time instants.

The L elements of column n of matrix A represent the transfer of the source strength at node n to the potentials of the L lead signals. The N elements of row l express the contributions of the N nodes to the potential at lead l . Matrix A incorporates all of the complexity of the volume conduction properties of the thorax.

Equation 1 is a general formulation that holds true as long as the transfer between sources and potentials at lead positions is independent of time. Here we will assume this to be the case.

The source type described is called the equivalent double layer (EDL). It is a completely general source description known from physics that allows a unique specification of potentials on the thorax by all sources active within an interior closed surface. In its application to the modeling of the ECG described in this article, the surface involved is S_h , and the time course of the local double-layer strength is linked to that of the local transmembrane potential.^{3,6-8}

Whenever the double-layer strength is uniform over S_h , the potential differences external to the double layer are zero, because S_h is a closed surface. This corresponds to the well-known fact that in a uniformly polarized state, myocardial cells do not produce an external field. An important consequence of this is that the sum of all elements of any row of the transfer matrix is zero. Expressed in matrix notation:

$$Ae = 0, \tag{2}$$

with e the unit vector of dimension N having elements of unit value only. Another implication is that the mean level of the instantaneous spatial distribution of the source strength does not affect the corresponding mean level of the potentials in the external medium. This allows one to shift the level of the transmembrane potential in the fully polarized state to zero, as is done in this article. The corresponding magnitude V_m of the upstroke of the transmembrane potential is scaled to a uniform value of 100 mV, being its order of magnitude.

For body surface potentials, Equation 2 signifies that their mean value is unspecified and, hence, some *ad hoc* value has to be assigned to it. In the standard 12-lead ECG, this value is the mean of the potentials at the left arm, right arm, and the left leg: the Wilson central terminal (WCT) reference. In this article, we apply a shift resulting in zero mean value of the potentials at all leads used: the zero mean reference (ZM).

In the implementation of the EDL source model, a uniform general shape $S(t)$ is assigned to the time course of the source strengths at all nodes on S_h . The time course used is the stylized transmembrane potential shown by the solid line in Figure 2. The particular waveform assigned to any node n is timed to reflect the local depolarization δ_n : the time of maximum slope of the local transmembrane potential.

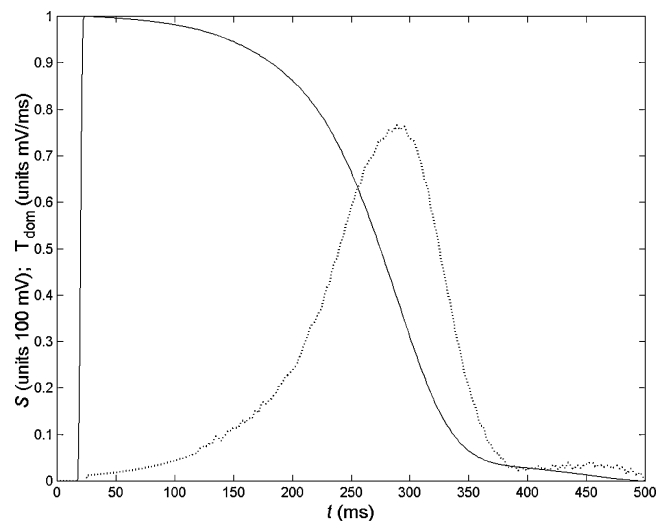


Figure 2. Solid line: Stylized version of a transmembrane potential; full scale 100 mV. Baseline shifted to zero. Dotted line: Derivative of the downstroke of the solid line, with inverted sign; full scale: 1 V/s = 1 mV/ms.

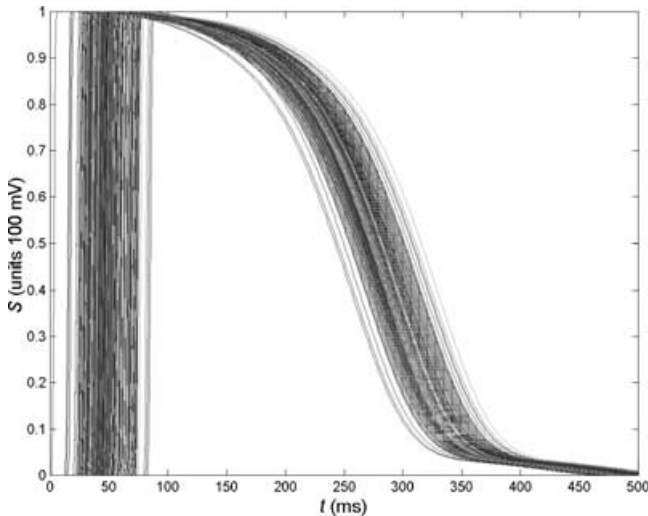


Figure 3. Collection of the (257) rows of the source strength matrix S . When applied to Equation 1 and used in combination with an appropriate forward transfer matrix A , this source strength faithfully reproduced the signals shown in Figure 1. Note that the dispersion of repolarization times is smaller than that of the depolarization times.

Similarly, the timing of local repolarization at node n is specified by ρ_n : the moment at which the magnitude of the downward slope of the transmembrane potential is maximal. For the time course of the source strength at node n , we write accordingly $S_n(t) = S(t; \delta_n, \rho_n)$. It is demonstrated in previous work³ that by specifying values for (δ_n, ρ_n) in combination with an appropriate volume conductor model, this source model is capable of generating accurate QRST waveforms. A complete set of $S_n(t)$ curves, like those used in a previous work,³ is shown in Figure 3. As a measure for the local action potential duration (APD), we use $\alpha_n = \rho_n - \delta_n$.

Defining the Dominant T Wave

The dominant T wave is introduced based on the analysis of a biophysical model. In the next section, it is shown how it can be computed from observed body surface potentials.

In this analysis, we concentrate on the electric potentials related to the repolarization currents only, for which we denote the source strength at the nodes n as $S_n(t) = S(t; \rho_n) = D(t - \rho_n)$, with $D(\cdot)$ the shape of the downward part of the solid line shown in Figure 2. The final part of this expression reflects the fact that a uniform shape is assumed for the source strength as a function of time, with its timing specified by ρ_n . For nodes at which repolarization arrives later, the curve of the source strength merely shifts to the right.

The repolarization times at all nodes differ: if they were equal, there would not be a T wave, as follows from Equation 2. The mean value of the repolarization times at the N nodes is denoted as $\bar{\rho}$. Accordingly we may write $\rho_n = \bar{\rho} + \Delta\rho_n$, with $\Delta\rho_n$ the individual differences from the mean. In statistical terms, the differences in the timing of repolarization at the N nodes, *viz.*, the dispersion of repolarization times, can be specified by either the range of the ρ_n values or their standard deviation. The latter is, of course, identical to the standard deviation of the $\Delta\rho_n$ values.

The next step of the analysis makes use of the fact that the duration of the downward slope is generally longer than the range of repolarization times as defined by the ρ_n values.

The duration of the downward slope may be taken as the time interval from 90% to 10% of the downward curve. This takes about 100 msec. In a previous article,³ it was shown from inverse computations that in healthy subjects the range of the repolarization times of the nodes is about 50 msec. This is in agreement with earlier invasive data shown by Franz et al.⁹ and Cowan et al.¹⁰ In Appendix A, it is shown that the time course of the source strength at node n with timing ρ_n can be approximated from the time course pertaining to the mean repolarization time value $\bar{\rho}$ as:

$$D(t - \bar{\rho} - \Delta\rho_n) \cong D(t - \bar{\rho}) - D'(t - \bar{\rho})\Delta\rho_n, \quad (3)$$

with D' denoting the time derivative of the downward slope $D(t - \bar{\rho})$. The approximation improves the smaller the shift $\Delta\rho_n$. It is demonstrated in Figure 4 that for a shift of as much as 20 ms applied to $D(t - \bar{\rho})$, the downward part of the solid line shown in Figure 2, the approximation is fair.

In the final step leading toward the introduction of the dominant T wave, we assume the range of $\Delta\rho_n$ values to be small compared to the duration of the downward slope, as discussed earlier. It is shown in Appendix B that under these conditions, $\psi_l(t)$, the potential during the ST-T segment at any lead l on the thorax, may be written as:

$$\psi_l(t) = w_l D'(t - \bar{\rho}), \quad (4)$$

in which $w_l = -\sum_n a_{l,n} \Delta\rho_n$, with $a_{l,n}$ denoting the elements of the transfer matrix A . The lead potential is denoted by ψ rather than by φ to stress that the potentials relate to repolarization only.

Equation 4 states that if the range of the repolarization times is very small, the shapes of the T waves of all leads on the thorax are identical: $D'(t - \bar{\rho})$, having amplitudes that are proportional to w_l , factors that are specific for each lead l . The factors w_l are linear combinations of the $\Delta\rho_n$ values, the individual differences from the mean of the repolarization times at the nodes n . The elements $a_{l,n}$ of row l of the transfer matrix A form this linear combination. Its outcome

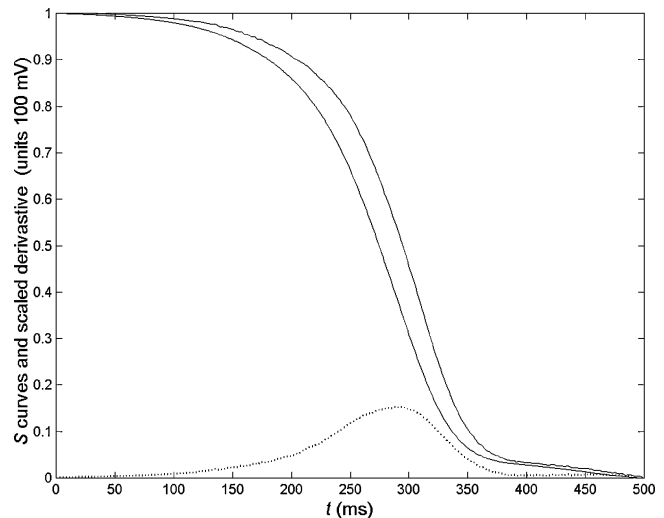


Figure 4. Shift invoked by adding a scaled derivative. Left downsloping solid line: Downslope of the shape shown in Figure 2. Dotted line: Derivative of the downward curve multiplied by -20 (ms). Right solid line: Sum of the left solid line and the dotted line. Note that the right solid line approximates the left one but for a shift of 20 ms.

determines the amplitude and sign of w_l and, hence, the amplitude and sign of the T wave in lead l .

Based on the preceding analysis, the dominant T wave, T_{dom} , is defined as:

$$T_{\text{dom}}(t) = -D'(t - \bar{\rho}), \quad (5)$$

the time derivative of the part of the transmembrane potential during repolarization. The negative sign is inserted to force the apex of T_{dom} to be positive. The shape of $T_{\text{dom}}(t)$ is that of the dotted line shown in Figure 2. Its peak value is about 0.75 V/s ($= 0.75 \text{ mV/msec}$). Its dimension reflects it being a derivative with respect to time.

Methods

Estimating the Dominant T Wave

Now that the dominant T wave has been defined, it will be shown how it can be estimated from observed ECGs. Throughout, the analysis remains within the framework of the modeling assumptions implied earlier, a uniform shape of the downward part of the transmembrane potential $D(t)$, and extreme values of $\Delta\rho_n$ that are small compared to the duration of the downward slope. Under these conditions, the dominant T wave in fact completely “dictates” the shape of the observed T waves. The QRST segment is divided into two intervals, separated by the J point, with its timing denoted as t_J . Beyond t_J , repolarization currents exclusively specify the observed potentials; prior to t_J , there is a mixture of depolarization- and repolarization-related currents.

Several heuristic methods have been proposed in the literature for the identification of t_J from observed body surface potentials, a problem that does not have a unique solution. In the present study, it was identified from the $\text{RMS}(t)$ curve, with $\text{RMS}(t)$ being the root mean square value of the potentials at time instant t computed over all leads involved. In particular, when using the ZM reference, as was done in this study, the $\text{RMS}(t)$ curve exhibits a clear local minimum at the end of the QRS complex. This point in time was taken to be t_J .

The Final Part of the Curve

The observed signals, data matrix Φ , were copied to a matrix Ψ . The first t_J columns of this matrix were assigned zero values. In this way, the elements of Ψ relate to repolarization currents only. Next, for each of the rows of Ψ , a summation of its elements was performed. This results in values that are proportional to the so-called ST-T integrals, one for each of the observed L lead signals. These values are used as weights of the respective leads while computing a weighted mean of the observed lead signals. For an upright T wave in any lead, the ST-T integral is positive and, hence, so is the factor weighting its contribution to the mean. For a negative T wave, its weight also is negative and, hence, the scaled version is upright. Biphasic T waves attain relatively small weights. The weighted mean waveform resulting from the application of this procedure, applied to the signals shown in Figure 1, is shown in Figure 5 (solid line segment only). Appendix C describes the background of this procedure. Note that, because the observed signals were referred to zero mean, a straightforward averaging of the ST-T signals would result in a curve that is zero.

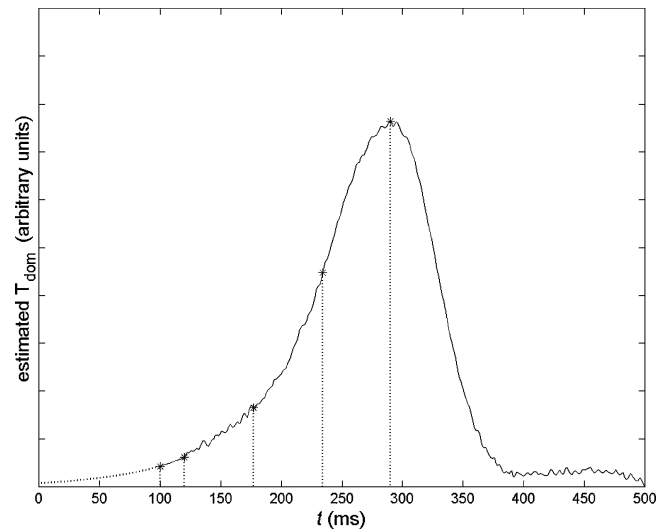


Figure 5. Shape of the dominant T wave as estimated from 64 QRST waveforms of a healthy subject. Solid line: Weighted mean of the signals beyond the J point. Dashed line: Extrapolation down to $t = 0$. Dashed vertical lines mark, from left to right, the time points used in the extrapolation: t_1 , t_2 , t_3 and t_{apex} (see Appendix D).

The Leading Part

The solid line segment in Figure 5 has a waveform that is similar to that of the dotted line shown in Figure 2. The vertical scale of Figure 5 is, deliberately, unspecified. (The scaling is discussed in the next paragraph.) The procedure described earlier leaves the curve up to t_J unspecified. During this interval, the observed potentials are dominated by depolarization-related currents, and, inevitably, all values of the leading part of the curve, the dotted part, are “speculative.” The specification of the leading part of the curve, as presented later, was inspired by an examination of the body surface potentials of 150 subjects (normal subjects and various patient categories) recorded during a previous study.¹¹ The study used data collected by a 64-lead system.¹² For all subjects, the procedure applied to observed ST-T signals resulted in weighted mean waveforms of the type depicted by the solid line shown in Figure 5. An analysis of the weighted mean signals of these subjects indicated that the early part of the ST-T waveforms could be represented accurately by means of an exponential curve. This observation was used to estimate (by means of extrapolation) the shape of part of the curve during the interval leading up to t_J . The parameters of the exponential function were computed from three values of the initial part of the mean signal, taken at equal time intervals. Details of this computation are given in Appendix D. The resulting extrapolation is indicated by the dotted line in Figure 5.

The Scaling

The complete waveform shown in Figure 5 was taken to be that of $T_{\text{dom}}(t)$. The scaling of this waveform was done as follows. Because $T_{\text{dom}}(t)$ is the derivative of $-D(t - \bar{\rho})$, the integral over time of $-D'(t - \bar{\rho})$ is equal to 100 (mV), being the maximum value of $D(t - \bar{\rho})$, the function shown in Figure 2. As a consequence, the required scaling of the curve shown in Figure 5 is performed easily by scaling it such that

its integral over time is indeed 100 mV. The shape of $T_{dom}(t)$ resembles that of a positive T wave as observed on the body surface.

Results

After having sampled the ECG signals and having stored the samples in a computer memory, the computation of $T_{dom}(t)$ is a straightforward procedure. In Figures 1 to 6, the data matrix involved was based on $L = 64$ observed lead signals, sampled at $T = 500$ points at 1-msec intervals. The matrix manipulations required to compute $T_{dom}(t)$ take <1 second.

Figure 6 depicts a set of computed dominant T waves. These are derived from the 64 signals recorded in a previous study.¹¹ The curves shown in Figure 6 are derived from the data of three healthy subjects, as well as from three cases listed in the study as old myocardial infarctions (MIs).

In healthy subjects, the value of T_{dom} at the J point, $t = t_J$, is small, reflecting the small slope of the TMP during phase 2 of repolarization. A related property is that, because the total integral over time of $T_{dom}(t)$ is fixed (100 mV), in healthy subjects the width of $T_{dom}(t)$ can be expected to decrease if its amplitude increases. This idea was tested by plotting w_h , the half-width of T_{dom} , as a function of $T_{dom}(t_{apex})$ as observed in the 50 healthy subjects. The half-width was taken to be the interval spanning two points on the $T_{dom}(t)$ curve, one to the left and the other to the right of the apex of T_{dom} , positioned at values $1/2 T_{dom}(t_{apex})$. The result is shown in Figure 7. The solid line shown depicts the hyperbolic function $w_h \times T_{dom}(t_{apex}) = const$, with $const = 86.6$ mV, being the mean value of the 50 observed $w_h \times T_{dom}(t_{apex})$ values. The other basic statistics involved were (mean \pm SD) $T_{dom}(t_{apex}) = 0.786 \pm 0.097$ mV/msec and $w_h = 111.8 \pm 15.0$ msec.

When the procedure for estimating T_{dom} was applied to just the subset of eight independent signals among the standard 12-lead ECG (V_1-V_6 , V_R , and V_L), the resulting $T_{dom}(t)$ waveforms were essentially the same. This is illustrated in Figure 8, a scattergram of the $T_{dom}(t_{apex})$ values of the 50 healthy subjects based on 64 leads and on the 8 leads. The linear correlation coefficient of these two variables was 0.98. The other statistics involved were (mean \pm SD) $T_{dom}(t_{apex})$

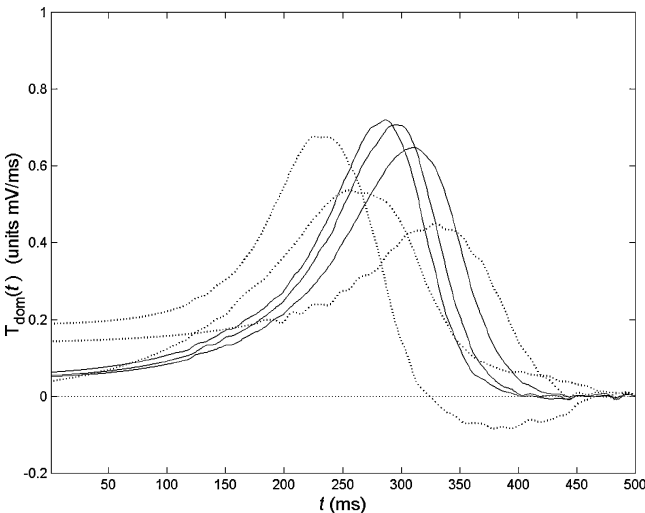


Figure 6. Selected dominant T waves. Solid lines: Three healthy subjects. Dashed lines: Three cases of old myocardial infarction.

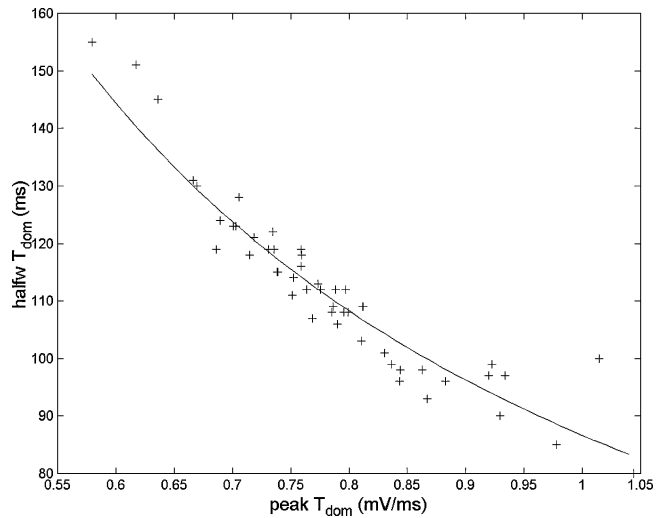


Figure 7. Scattergram of $T_{dom}(t_{apex})$ and the half-width w_h as derived from 50 healthy subjects. Solid line depicts the function $w_h \times T_{dom}(t_{apex}) = 86.6$ mV. See text for the significance of this function.

(8 leads) = 0.782 ± 0.100 mV/msec and $T_{dom}(t_{apex})$ (64 leads) = 0.786 ± 0.096 mV/msec.

Negative values of $T_{dom}(t)$, appearing only during the final part of the ST-T interval, were found exclusively in patient data. An example of this is shown by one of the dashed lines in Figure 6.

Discussion

The dominant T wave $T_{dom}(t)$, as introduced in this article, can be interpreted as representing the temporal behavior of the slope of a “mean” type of transmembrane potential (TMP) involved in the genesis of the ECG. The assumption involved in the formulation of the background to the dominant T wave may appear to be unrealistic: “real” TMP potentials may not all have an identical shape during repolarization and the dispersion of the timing repolarization may be large, particularly in cases of disease. However, even if the dispersion is large,

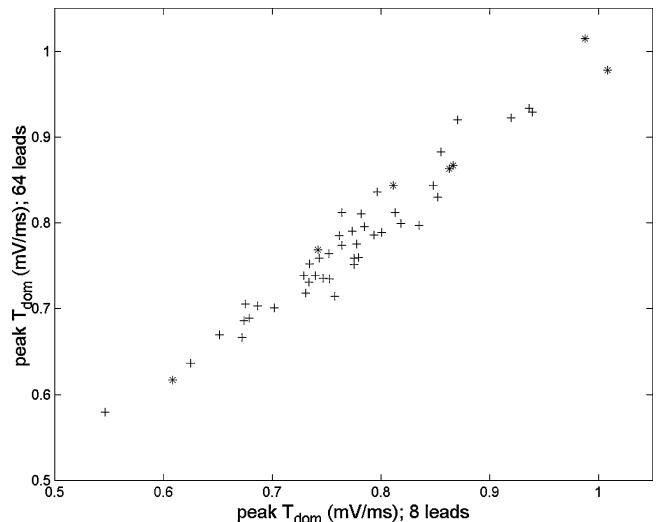


Figure 8. Scattergram of $T_{dom}(t_{apex})$ values estimated from 64 leads and those derived from eight leads in 50 healthy subjects, seven of whom (asterisks) were females.

the model has been found to be capable of simulating biphasic T waves on the ECG. The presence of such waveforms on the ECG has relatively small effect on the estimation of T_{dom} : the specific weighted mean used proved to be a robust estimator. The assumption of a uniform “mean” shape of the downslope is a very strong, first-order approximation. The effect of deviations from this mean shape (the second-order terms) has been found to produce only relatively small differences in the ECG.

Properties of T_{dom}

Because $T_{dom}(t)$ is the gradient of a TMP, its amplitude is independent of volume conduction effects: the effects of the passive tissues surrounding the heart. Because of this, differences in body size and heart position do not affect its amplitude. Computing $T_{dom}(t)$ does not require solving an inverse problem. This is a property that is maintained in its estimated variant, owing to the scaling based on its integral over time. This is a unique feature, not shared by any other magnitude feature of the potentials recorded on the body surface.

In healthy subjects, the value of T_{dom} at the J point $t = t_j$ is small, reflecting the small slope of the TMP during phase 2 of repolarization. For types of disease in which the TMP slope during phase 2 of repolarization is substantial, the value of $T_{dom}(t)$ at the J point, $T_{dom}(t_j)$, is expected to be larger than in healthy subjects. This was confirmed by comparing its mean value in the healthy subjects to those of all patient categories contained in the database. This was found to be true, particularly for the old MI and angina patients. In two of the old MI cases shown in Figure 6, clearly elevated ST segments are shown. For some of the old MI patients, the elevation was less apparent, probably indicating a more complete healing over at the boundary of the infarcted area. An illustration of this is the middle of the three dashed curves shown in Figure 6.

The extension of the dominant T wave, stretching into the QRS interval as carried out by means of the exponential function (Appendix D), was used in this work merely to make sure that the scaling of $T_{dom}(t)$ by means of its integral over time makes sense in the presence of elevated $T_{dom}(t_j)$ values. However, it does focus the attention on the possible mixing of depolarization currents and repolarization currents during QRS, particularly if phase 2 of the TMP is steep.

Analysis as such indicates how the ST-T elevation seen in $T_{dom}(t)$ is linked to phase 2 of the TMP. The current clinical interpretation of the ST-T slope as such in common T waves remains an open question. The shape of $T_{dom}(t)$ during the time interval between the J point and the timing of the apex could be fitted well by an exponential function. As such, there is no single constant slope value that can be used to quantify it. The parameter c as identified in Appendix D seems to be more appropriate to specify this part of the curve.

In healthy subjects, the waveform of $T_{dom}(t)$ was almost identical to that of the dominant signal (principal component) identified by means of the singular value decomposition of the observed Ψ data. Correlations of >99.5% were found in all cases. In most of these cases, the shape of $T_{dom}(t)$ was also very similar to that of the corresponding part of the RMS(t) curve beyond $t = t_j$. Here the differences were larger, mainly in the cases where both the dominant singular signal and

$T_{dom}(t)$ were negative: by its nature, RMS(t) is always positive.

The peak value of $T_{dom}(t)$ reflects the maximum downward slope of the TMP. It was found in a previous study³ that the timing of the peak coincided with the mean of the inversely computed repolarization times ρ_n . This also can be seen in the results shown in the early model-based study by Harumi et al.⁴ An important experimental confirmation of the same fact can be found in the study by Fuller et al.¹³ Figure 5b of their article shows that the timing of the peak of the RMS(t) curve was the same as the mean repolarization time on the epicardium as observed under a wide diversity of experimental conditions. This provides confirmation because in the present material the timing of apex of $T_{dom}(t)$ of apex RMS(t) was essentially the same.

An interactive simulation package that uses $T_{dom}(t)$ in the simulation of $T_{com}(t)$ recently has been made available on the Internet (www.ecgsim.com).¹⁴ This package can be used to study the expression of $T_{dom}(t)$ on body surface potentials.

Conclusion

The dominant T wave as introduced in this article forms the theoretical link between gross cellular behavior of the myocardium and the common T waveforms that result. In itself, the dominant T wave has properties that seem to be worthwhile for inclusion in diagnostic procedures. It is the only waveform with an amplitude that is unaffected by volume conduction effects.

Appendices

Appendix A

Equation 3 follows from the application of the Taylor expansion, a tool well known from mathematics. Applied to $D(t - \bar{\rho} - \Delta\rho_n)$ and small values of $\Delta\rho_n$, this expansion reads:

$$D(t - \bar{\rho} - \Delta\rho_n) = D(t - \bar{\rho}) + \frac{\partial D(t - \bar{\rho})}{\partial \bar{\rho}} \Delta\rho_n + \dots \quad (A1)$$

The specific nature of the D allows one to write $\frac{\partial D(t - \bar{\rho})}{\partial \bar{\rho}} = -\frac{\partial D(t - \bar{\rho})}{\partial t}$; hence, we have:

$$D(t - \bar{\rho} - \Delta\rho_n) \cong D(t - \bar{\rho}) - \frac{\partial D(t - \bar{\rho})}{\partial t} \Delta\rho_n. (= \text{Equation 3})$$

q.e.d.

The approximation involved results from using just the two leading terms of the expansion. For larger values of the shift, subsequent terms in the Taylor expansion need to be included.² Here we use just the leading two terms.

Appendix B

Proof of Equation 4. The first term on the right in Equation 3, the function $D(t - \bar{\rho})$, is identical for all nodes n . Similarly, in the second term, the function $D'(t - \rho) = \frac{\partial D(t - \bar{\rho})}{\partial t}$ is identical for all nodes. Based on Equation 1, the potential

during the ST-T segment at any lead l on the thorax may be written as:

$$\begin{aligned}\psi_l(t) &= \sum_n a_{l,n} s_{n,t} = \sum_n a_{l,n} D(t - \bar{\rho} - \Delta\rho_n) \\ &= \sum_n a_{l,n} (D(t - \bar{\rho}) - D'(t - \bar{\rho}) \Delta\rho_n) \\ &= -\sum_n a_{l,n} D'(t - \bar{\rho}) \Delta\rho_n.\end{aligned}$$

The term pertaining to $D(t - \bar{\rho})$ vanishes because of Equation 2; thus, the final result reads:

$$\begin{aligned}\psi_l(t) &= -\sum_n a_{l,n} D'(t - \bar{\rho}) \Delta\rho_n \\ &= (-\sum_n a_{l,n} \Delta\rho_n) D'(t - \bar{\rho}) = w_l D'(t - \bar{\rho}),\end{aligned}$$

with $w_l = -\sum_n a_{l,n} \Delta\rho_n$, q.e.d.

Appendix C

The motivation for estimating the dominant T wave as a weighted mean of the observed ST-T signals is as follows. The starting point is Equation 4, which in matrix notation reads:

$$\Psi = \mathbf{w} \mathbf{d}^t, \quad (\text{C1})$$

with column vector \mathbf{w} specified by $\mathbf{w} = -\mathbf{A} \Delta\rho$ and \mathbf{d}^t a row vector denoting the major part of the dominant T wave beyond t_J . Recall that Ψ relates to signals during this time interval only. We now introduce the ST-T integrals of all observed lead signals, which can be approximated numerically by adding up all samples of the observed lead potential. In matrix notation:

$$\mathbf{i} = \Psi \mathbf{e}, \quad (\text{C2})$$

with \mathbf{i} a column vector representing the ST-T integrals and \mathbf{e} a column vector having elements 1 only. By post-multiplying Equation C1 by \mathbf{e} , we find that:

$$\Psi \mathbf{e} = \mathbf{w} \mathbf{d}^t \mathbf{e}. \quad (\text{C3})$$

The nature of $\mathbf{d}^t \mathbf{e}$ is that of a scalar, denoted here by β , whose value remains undetermined. From Equation C3 we see that $\mathbf{w} = \Psi \mathbf{e} / \beta$. We now pre-multiply both sides of Equation C1 by $\mathbf{w}^t = \mathbf{e}^t \Psi^t / \beta$, yielding:

$$\mathbf{e}^t \Psi^t \Psi / \beta = \mathbf{w}^t \mathbf{w} \mathbf{d}^t, \quad (\text{C4})$$

and we observe that $\mathbf{w}^t \mathbf{w}$ is an (unknown) scalar, denoted by α . The final result demonstrates that the major part of the dominant T wave can be estimated as:

$$\mathbf{d}^t = \mathbf{e}^t \Psi^t \Psi / (\alpha \beta), \quad (\text{C5})$$

a function that is specified up to a scaling factor. The determination of this factor follows from demanding its integral over time to be equal to be 100 mV, the value used in this article to specify V_m , as discussed in the main text. Note that the values of α and β need not be known.

Also note that the weighing factors $\mathbf{w} = \Psi \mathbf{e} / \beta$ involved in computing the weighted mean of the ST-T signals are proportional to the ST-T integrals of the corresponding lead signals.

Appendix D

The method for extrapolation of the dominant T wave down to its initial part uses the exponential function:

$$y(t) = a + b e^{ct}. \quad (\text{D1})$$

This function is specified by the three parameters a , b , and c . Generally, determination of these parameters requires the solution of a nonlinear parameter estimation problem. However, for the problem in hand, inspection of the data revealed that the weighted mean waveforms were largely noise-free, and—as became evident from the tests based on the patient data—all curves closely followed the function described in Equation D1. Moreover, because the function was to be used only for extrapolation during the interval up to the timing of the J point, t_J , a direct computation of the parameters was used. To this end, three equidistant points in time, t_1 , t_2 , and t_3 , were selected in the interval between t_J and t_{apex} , the timing of the peak of the weighted mean curve. The first point, t_1 , was placed 20 msec to the right of t_J as identified by the local minimum in the RMS(t) curve, in order to minimize the possibility of interference by late depolarization. The second point, t_2 , was placed further to the right. Its distance to t_1 , τ , was put at 30% of the interval from t_J to t_{apex} . A further shift to the right over the same distance τ specifies t_3 . This leaves t_3 well clear of the peak where, clearly, the function specified in Equation D1 does not apply. By using an equal distance τ between the three points in time, the parameters (a , b , c) can be computed directly from the function values (y_1 , y_2 , y_3), as shown below.

$$\text{Let } t_1 = t_2 - \tau, \quad \text{and } t_3 = t_2 + \tau.$$

By using $y_2 - y_1 = b e^{ct_2} (1 - e^{-c\tau})$ and $y_3 - y_2 = b e^{ct_2} (e^{c\tau} - 1)$, and by denoting $(y_3 - y_2) / (y_2 - y_1) = \alpha$, as well as $e^{c\tau} = x$, a quadratic equation emerges: $\alpha = \frac{x-1}{1-1/x}$, having as a relevant solution $x = \alpha = e^{c\tau}$. Hence,

$$c = \frac{\ln(\alpha)}{\tau}, \quad b = \frac{y_3 - y_2}{e^{ct_2} (e^{c\tau} - 1)}, \quad \text{and } a = y_2 - b e^{ct_2}.$$

Acknowledgments: The author acknowledges gratefully the careful reading of this manuscript and the ensuing corrections by T.F. Oostendorp, J.I. van Oosterom-Pooley, and M.M. van Pelt.

References

1. De Ambroggi L, Aime E, Ceriotti C, Rovida M, Negroni S: Mapping of ventricular repolarization potentials in patients with arrhythmogenic right ventricular dysplasia. *Circulation* 1997;96:4314-4318.
2. van Oosterom A: Singular value decomposition of the T wave: Its link with a biophysical model of repolarization. *Int J Bioelectromagn* 2003;4:59-60.
3. van Oosterom A: Genesis of the T wave as based on an equivalent surface source model. *J Electrocardiol* 2001;34S:217-227.
4. Harumi K, Burgess MJ, Abildskov JA: A theoretic model of the T wave. *Circulation* 1966;XXIV:657-668.
5. van Oosterom A, Windau G, Huiskamp GJM: Simulation on a PC of the QRS-T wave forms. In Macfarlane PW, Rautaharju P, eds: *Electrocardiology '93*. Singapore: World Scientific, 1994, pp. 97-100.
6. Geselowitz DB: On the theory of the electrocardiogram. *Proc IEEE* 1989;77:857-876.
7. Geselowitz DB: Description of cardiac sources in anisotropic cardiac muscle. Application of bidomain model. *J Electrocardiol* 1992;25S:65-67.
8. di Bernardo D, Murray A: Explaining the T-wave shape in the ECG. *Nature* 2000;403:40.
9. Franz M, Bargheer K, Rafflenbeul W, Haverich A, Lichtlen P: Monophasic action potential mapping in a human subject with normal electrograms: Direct evidence for the genesis of the T wave. *Circulation* 1987;75:379-386.

10. Cowan JC, Hilton CJ, Griffiths CJ, Tansuphaswadikul S, Bourke JP, Murray A, Campbell RWF: Sequence of epicardial repolarisation and configuration of the T wave. *Br Heart J* 1988;60:424-433.
11. Uijen GJH, Heringa A, van Oosterom A, van Dam RT: Body surface maps and the conventional 12-lead ECG compared by studying their performances in classification of old myocardial infarction. *J Electrocardiol* 1987;20:193-2002.
12. Heringa A, Uijen GJH, van Dam RT: A 64-channel system for body surface potential mapping. In Antalóczy Z, Préda I, eds: *Electrocardiology 1981*. Budapest, Hungary: Academia Kiado, 1982, pp. 297-297.
13. Fuller MS, Sandor G, Punske B, Taccardi B, MacLeod RS, Ershler PR, Green LS, Lux RL: Estimates of repolarization and its dispersion from electrocardiographic measurements: Direct epicardial assessment in the canine heart. *J Electrocardiol* 2000;33:171-180.
14. van Oosterom A, Oostendorp TF: ECGSIM: An interactive tool for studying the genesis of QRST waveforms. *Heart* 2003;(In press).